International Journal of Applied Mathematics
Volume 38 No. 3s, 2025
ISSN: 1311-1728 (printed version); ISSN: 1314-8060 (on-line version)

CRISIS COMMUNICATION ON SOCIAL MEDIA: POSSIBILISTIC REASONING OVER INCOMPLETE EVIDENCE

Suleiman Ibrahim Shelash Mohammad[1,2], Yogeesh N[3*], N Raja[4], Hanan Jadallah[5], Aliyaparveen Mulla[6], Divakara K[7], Asokan Vasudevan[8,9], Shankaralingappa B M[10]

[1] Electronic Marketing and Social Media, Economic and Administrative Sciences Zarqa University, Zarqa 132010, Jordan

[2] Research follower, INTI International University, Negeri Sembilan 71800, Malaysia

Email: dr_sliman@yahoo.com, ORCID ID: 0000-0001-6156-9063

[3] Department of Mathematics, Government First Grade College, Tumkur, Karnataka, India. Email: yogeesh.r@gmail.com ORCID ID: orcid.org/0000-0001-8080-7821

[4] Department of Visual Communication, Sathyabama Institute of Science and Technology, Chennai, Tamil Nadu, India. Email: rajadigimedia2@gmail.com, ORCID: 0000-0003-2135-3051

5 Electronic Marketing and Social Media, Economic and Administrative Sciences Zarqa University, Zarqa 132010, Jordan

Email: Hananjadallah1987@gmail.com, ORCID ID: 0009-0005-7138-1167

[6] Department of English, Government First Grade College Managuli Dist Vijayapur, India. Email: aaliyaparveen777@gmail.com

[7] Department of Political Science, Government First Grade College Thyamagondlu -562132, Bangalore Rural (Dist), India. Email: kdivakara25@gmail.com, ORCID: https://orcid.org/0009-0006-7648-3661

[8]Faculty of Business and Communications, INTI International University, Nilai 71800, Malaysia

[9]Faculty of Management, Shinawatra University, 99 Moo 10, Bangtoey, Samkhok 12160, Thailand
asokan.vasudevan@newinti.edu.my

[10] Department of Mathematics, Government First Grade College for Women, M G Road, Hassan-573201, India. Email: shankar.gsch@gmail.com, ORCID: https://orcid.org/0000-0001-8121-2715

***Corresponding author:** yogeesh.r@gmail.com

Abstract

This study presents a mathematically grounded framework for decision-making when digital reports are fragmentary, delayed, or conflicting. We formulate an ordinal approach in which social signals are mapped to fuzzy predicates and encoded as constraints that induce least-

Received: July 20, 2025

International Journal of Applied Mathematics
Volume 38 No. 3s, 2025
ISSN: 1311-1728 (printed version); ISSN: 1314-8060 (on-line version)

committal distributions. Heterogeneous cues are combined with t-norm/t-conorm operators (default max–min), and time evolution is handled by a max–min convolutional filter with bounded drift. Information spread and credibility are modeled on interaction graphs via a trust-weighted diffusion operator that is monotone and admits a least fixed point. Operational triggers are cast as threshold rules on dual statistics necessity for conservative guarantees and possibility for coverage supported by complexity-aware algorithms and theoretical properties (monotonicity, non-expansiveness, and fixed-point existence). Experimental design uses event-wise splits, ordinal metrics (guaranteed precision vs. alert rate, coverage width), and ablations over fusion families, kernel bandwidth, and trust decomposition. A flood-onset case study demonstrates timely alerts under missing cues, while a public-health rumor scenario shows transparent containment dynamics and rapid convergence. Across scenarios, necessity-based alerts achieve high guaranteed precision at controllable alert rates, with tunable lead time and auditable contributions from cues, rules, and trust links. The framework provides a practical substrate for ethically governed operations, and a foundation for future hybrid probabilistic-ordinal models and learned encoders.

Keywords: ordinal uncertainty; max–min fusion; t-norm aggregation; temporal filtering; trust-weighted diffusion; rumor containment; decision thresholds; imprecise probability.

1. Introduction

1.1 Problem Context & Motivation

1.1.1 *Crisis communication on social platforms under uncertainty*

During fast-evolving crises (floods, epidemics, industrial accidents), responders must interpret incomplete, noisy, and conflicting social-media signals to decide **when** to alert, **what** to prioritize, and **where** to dispatch resources. Classical probability needs precise likelihoods that are often unavailable in early crisis minutes; instead, *possibility theory* provides ordinal, set-based bounds well-suited to partial evidence and imprecision [1,2]. It enables reasoning with *what is compatible* with observations (possibility) and *what is guaranteed* by them (necessity), which aligns with operators' need for conservative triggers in the presence of missing data [1,2–4].

Let Ω denote interpretations of the current crisis state (e.g., severity, location, misinformation status). A possibility distribution $\pi: \Omega \to [0,1]$ rates each $\omega \in \Omega$ by plausibility. The possibility measure and its dual necessity measure are

$$\Pi(A) = \sup_{\omega \in A} \pi(\omega),\ N(A) = 1 - \Pi(A^{C}) \qquad ---(1)$$

providing upper/lower ordinal bounds on event (e.g., "severity is high near Tumkur") [1,2].

1.1.2 Why possibility theory for incomplete/partial evidence

Social posts supply fragmentary predicates-e.g., "water above knee," "sirens heard," or "smell of gas"that can be encoded as fuzzy sets with membership $\mu \in [0,1]$ (for degree of support), from which π is derived by maximum specificity [1,2]. Possibilistic fusion via max-min operators tolerates missing features, avoids over-commitment, and yields monotone updates as

International Journal of Applied Mathematics
Volume 38 No. 3s, 2025
ISSN: 1311-1728 (printed version); ISSN: 1314-8060 (on-line version)

more evidence arrives [1,2,9,10]. This paper formalizes a crisis-ops pipeline grounded in (1), t-norm/t-conorm aggregation, and dioid algebra for temporal and network diffusion [6-9].

1.2 Contributions

We propose a math-centric framework for *Crisis Communication on Social Media: Possibilistic Reasoning over Incomplete Evidence* with these contributions:

1.2.1 *A possibilistic evidence model for crisis signals*

Given feature extractors $f \in \mathcal{F}$ (e.g., geotag confidence, urgency lexicon, source credibility), each observation x_f is mapped to a membership $\mu_f(x_f) \in [0,1]$. We define evidence-conditioned distributions π_f and fuse them using t -norm/ t -conorm families:

$$\pi_\wedge(\omega) = \min_{f\in\mathcal{F}} \pi_f(\omega),\ \pi_\vee(\omega) = \max_{f\in\mathcal{F}} \pi_f(\omega) \qquad ---(20$$

1.2.2 Temporal and network diffusion with max-min algebra

We model state evolution by a transition possibility kernel $M(\omega' \to \omega) \in [0,1]$ and update via the possibilistic filter:

$$\pi_t(\omega) = \max_{\omega'\in\Omega} \min(M(\omega' \to \omega), \pi_{t-1}(\omega'), e_t(\omega)) \qquad ---(3)$$

where encodes time- evidence [2,9,10]. On a trust-weighted interaction graph $= (,)$ with $\tau_{uv} \in [0,1]$, diffusion iterates

$$\pi^{(k+1)} = \max(\pi^{\text{self}}, \max_{u\in N(v)} \min(\tau \quad, \pi^{(k)})) \qquad ---(4)$$

which is a monotone map with a least fixed point in a complete lattice (via Tarski), implementable in the (max, min) dioid [9,10].

1.2.3 Decision rules using necessity/possibility thresholds

Operational triggers use necessity for conservative alerts and possibility for coverage:

$$\text{ALERT if } N_t(H) \geq \tau_N;\ \text{ DEFER if } \Pi_t(H) < \tau_\Pi\,. \qquad ---(5)$$

Weights for multi-criteria can be set using OWA or Sugeno integrals under ordinal information [6,7].

Figure 1. -Cuts of a Triangular Membership Function for Crisis Severity

Received: July 20, 2025

International Journal of Applied Mathematics
Volume 38 No. 3s, 2025
ISSN: 1311-1728 (printed version); ISSN: 1314-8060 (on-line version)

This figure 1 illustrates a triangular membership $\mu_{\text{severity}}(x)$ with support [2,9] and peak at 6. Horizontal lines mark α-cuts for $\alpha \in \{0.2, 0.5, 0.8\}$. The interval $[L_\alpha, U_\alpha]$ is obtained analytically as $L_\alpha = a + \alpha(b-a), U_\alpha = c - \alpha(c-b)$. a-cuts drive ordinal set operations for computing Π and N from fuzzy descriptors in early-crisis evidence encoding [1,2].

2. RELATED WORK

2.1 Probabilistic and Dempster–Shafer (DS) approaches

Probabilistic models require calibrated likelihoods and priors, which are scarce early in a crisis; DS theory represents belief mass on sets and yields belief/plausibility bounds but can become computationally heavy with non-consonant focal sets [5]. Consonant DS functions correspond to possibility measures, enabling ordinal upper/lower bounds compatible with linguistic evidence [1,2,5].

2.2 Fuzzy logic in social sensing

Fuzzy sets and linguistic variables model gradable predicates ("likely flood," "strong odor") with membership functions μ that capture vagueness rather than randomness [1]. Aggregation can be performed using **Ordered Weighted Averaging** (OWA) to encode optimistic/pessimistic attitudes [6] or with **Sugeno integrals** to respect ordinal scales and interaction among criteria [7]. When scarce cardinal information is available, **Choquet integrals** support non-additive aggregation guided by capacities, though they require more elicitation [8].

2.3 Possibility theory and possibilistic logic

Possibility theory provides a qualitative framework for **upper envelopes** Π and **guarantee levels** N with max–min calculus, supporting *cautious* crisis decisions under missing data [1,2]. **Possibilistic logic** attaches certainty weights to formulas (φ, w) and reasons by stratified entailment, controlling inconsistency via the *inconsistency degree* of the knowledge base useful when social signals conflict (e.g., rumor vs official) [2,11]. In our pipeline, rule-based detectors (e.g., "photos show *knee-deep water*") become weighted clauses contributing to e_t in (3).

2.4 Gaps in current crisis informatics

State-of-the-art crisis-informatics systems mine and classify messages, infer situational updates, and route information, predominantly with probabilistic or supervised learning paradigms that presume labeled data and stationarity [3,4]. Two persistent gaps motivate our approach:

(1) **Ordinal uncertainty with missingness.** Early streams contain *incomplete* and *imprecise* cues (e.g., vague locations), where ordinal compatibility is more defensible than precise probabilities [1–3].

(2) **Trust-aware diffusion under weak data.** Social propagation interacts with credibility; max–min network diffusion (4) offers monotone, data-efficient propagation with formal fixed-point guarantees in dioid algebraic settings [9,10], a niche not fully exploited by existing probabilistic graph methods [3,4].

Received: July 20, 2025

International Journal of Applied Mathematics
Volume 38 No. 3s, 2025
ISSN: 1311-1728 (printed version); ISSN: 1314-8060 (on-line version)

3. MATHEMATICAL PRELIMINARIES

3.1 Possibility Theory Basics

3.1.1 *Distributions and measures*

Let Ω be the set of crisis-state interpretations (e.g., severities × locations × needs). A possibility distribution $\pi: \Omega \to [0,1]$ induces the possibility and necessity measures

$$\Pi(A) = \sup_{\omega \in A} \pi(\omega),\ N(A) = 1 - \Pi(A^{C})\ (A \subseteq \Omega), \qquad ---(6)$$

with axioms $\Pi(\emptyset) = 0, \Pi(\Omega) = 1, \Pi(\bigcup_i A_i) = \sup_i \Pi(A_i)$ and dual properties for N[12,17]. When π is normalized ($\sup_\Omega \pi = 1$), $N(A \cap B) = \min(N(A), N(B))$ holds for crisp A, B [17].

3.1.2 Maximum-specificity principle

Given a set of constraints of the form $\Pi(A_j) \geq \alpha_j$, the least-committal (most specific) π consistent with them assigns

$$\pi(\omega) = \text{minmax}\,(\mathbf{1}_{\Omega \setminus A}\ (\omega), \alpha_j), \qquad ---(7)$$

which avoids unwarranted precision-crucial for sparse crisis signals [17].

3.1.3 -cuts and ordinal inference

For a fuzzy predicate F with membership $\mu_F: \Omega \to [0,1]$, the a-cut $F_\alpha = \{\omega: \mu_F(\omega) \geq \alpha\}$ links fuzzy evidence to set-based reasoning. Using (6), $\Pi(F) = \sup_\omega\ \mu_F(\omega)$ and $N(F) = \inf_{\alpha>0} \min(\alpha, 1 - \Pi(\Omega \setminus F_\alpha))$ in ordinal settings [12,15,17].

3.2 Fuzzy Numbers & L-R Shapes

3.2.1 Triangular/trapezoidal encodings

For a triangular $\tilde{x} = (a, b, c)$ (support $[a, c]$, peak at b), the membership is

$$\mu_{\tilde{x}}(x) = \begin{cases} \dfrac{x-a}{b-a}, & a \leq x \leq b \\ \dfrac{c-x}{c-b}, & b \leq x \leq c, \\ 0, & \text{otherwise} \end{cases} \quad {}^{\tilde{x}_\alpha} = [a + \alpha(b-a), c - \alpha(c-b)] \qquad ---(8)$$

Arithmetic on fuzzy numbers proceeds via -cut interval extension (compute on each interval, then recombine) [15].

3.2.2 L-R fuzzy numbers

General L-R numbers $\tilde{x} = (m; \ell, r; L, R)$ use shape functions L, R on left/right spreads and preserve order-level computations needed for crisis-severity scales [12,15].

3.3 Aggregation: t-Norms, t-Conorms, Integrals

3.3.1 t-norms and t-conorms

Received: July 20, 2025

International Journal of Applied Mathematics
Volume 38 No. 3s, 2025
ISSN: 1311-1728 (printed version); ISSN: 1314-8060 (on-line version)

A t-norm T: $[0,1]^2 \to [0,1]$ is commutative, associative, monotone, with $T(x,1) = x$; t-conorm dually satisfies $(\ ,0) =\ $. Canonical families:

$$T_{\min}(x,y) = \min(x,y),\ T_{\text{prod}}(x,y) = xy,\ T_{\text{Luk}}(x,y) = \max(0, x+y-1), \quad ---(9)$$

with dual S via De Morgan under a strong negation [13]. We adopt $T_{\min}, S_{\max}$ (Gödel pair) for cautious fusion, and optionally T_{Luk} for controllable compensation [13].

3.3.2 OWA and nonadditive integrals

For criteria $\{a_i\}$, an OWA aggregator uses sorted inputs $a_{(i)}$ and weights w_i with $\sum_i w_i = 1$:

$$\text{OWA}_w(a_1, \ldots, a_n) = \sum_{=1} w_i a_{(i)}, \qquad ---(10)$$

capturing optimism/pessimism in operator preference [18].

When interaction among criteria matters, we use Sugeno and Choquet integrals under capacities g on $2^{\{1,\ldots,n\}}$[14,19]:

$$\text{Sugeno}_g(a) = \text{maxmin}\ (a_{(i)}, g(A_{(i)}))\,, \quad \text{Choquet}_g(a) = \sum_{=1} (a_{(i)} - a_{(i-1)}) g(A_{(i)}), -(11)$$

where $A_{(i)} = \{(i), \ldots, (n)\}, a_{(0)} = 0$.

3.4 Possibilistic Logic

A weighted clause (φ, w) expresses that φ holds with certainty at least w. The inconsistency degree of a base $\mathcal{K}$ is the highest w such that $\mathcal{K} \vdash (\bot, w)$; stratified entailment filters conclusions above this level to manage conflicting social signals [20]. Necessity of a formula is computed by the lowest weight contradicting it, enabling robust rule-based crisis reasoning [21].

3.5 From Belief Functions to Possibility

Consonant Dempster-Shafer masses (nested focal sets) induce a possibility distribution

$$\pi(\omega) = \text{Pl}(\{\omega\}) = \sum_{A \ni \omega} m(A),\ \Pi(A) = \max_{\omega \in A} \pi(\omega) \qquad ---(12)$$

providing upper envelopes consistent with imprecise-probability views. This mapping justifies ordinal reasoning when only interval/confidence band information is extractable from posts [16,22].

Received: July 20, 2025

International Journal of Applied Mathematics
Volume 38 No. 3s, 2025
ISSN: 1311-1728 (printed version); ISSN: 1314-8060 (on-line version)

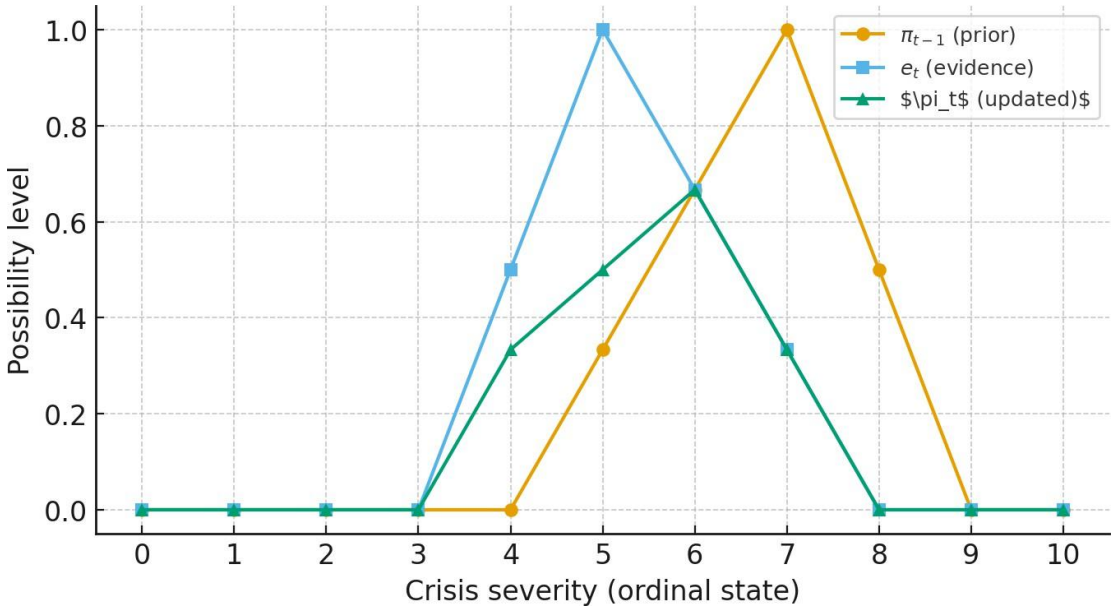

Figure 2. Possibilistic Temporal Update via Max-Min Convolution

We demonstrate Eq. (3) over a 1-D severity lattice: prior π_{t-1} peaked at 7, evidence e_t peaked at 5, and a triangular transition kernel allowing ± 2 severity change (See the figure 2). The updated distribution π_t arises from a maxmin "convolution," illustrating conservative drift toward the new evidence under bounded dynamics [12,13].

4. PROBLEM FORMULATION

Crisis Tasks: We formalize three operator tasks over social-media streams:

Detection/triage: Decide if a crisis on is ongoing and estimate ordinal severity.

Rumor verification: Assess whether a claim true (e.g., "bridge collapsed") is supported/contradicted.

Resource prioritization: Rank areas { } by necessity of need (need in) for dispatch planning.

4.2 Observation & Evidence Model

4.2.1 Social-post representation

Each post $o = (t, \ell, s,$ text, m) includes time t, fuzzy location ℓ, source s, lexical/vision features, and metadata m. Feature extractors (lexicons, georesolution, image cues) output $x_f \in \mathcal{X}_f$ and membership scores $\mu_f(x_f) \in [0,1]$ for predicates such as water depth, crowd panic, or smoke density [22,23].

4.2.2 Incomplete evidence and missingness

Let $\mathcal{F}_t$ be features observed at time t. For missing $f \notin \mathcal{F}_t$, we adopt the vacuous constraint $\Pi(\Omega) \geq 1$, which leaves π unchanged. Evidence is summarized as

Received: July 20, 2025

International Journal of Applied Mathematics
Volume 38 No. 3s, 2025
ISSN: 1311-1728 (printed version); ISSN: 1314-8060 (on-line version)

$$e_t(\omega) = \bigodot_{f \in \mathcal{F}_t} \pi_f(\omega), \text{ with } \odot \equiv T(\text{ default } T = \min), \quad ---(13)$$

where results from mapping to compatibility with state (e.g., severity component of consistent with the a-cut implied by)[12,15].

4.3 Hypothesis Space & State

4.3.1 Ordinal product lattice

Define the crisis state at time as

$$S_t = (\sigma_t, \lambda_t, \nu_t, \rho_t) \in \mathcal{S} = \Sigma \times \mathbf{\Lambda} \times \mathcal{N} \times P, \quad ---(14)$$

where $\Sigma =$ ordinal severities, $\mathbf{\Lambda} =$ location zones, $\mathcal{N} =$ need levels, $P =$ rumor polarity. We use the product partial order and pointwise max-min operations to propagate possibility across components [12,13].

4.3.2 Hypotheses

A hypothesis (e.g., "high severity in zone Z within 2 h") defines a crisp set $H \subseteq \mathcal{S}$ or a fuzzy set with membership μ_H. The decision statistics are

$$\Pi_t(H) = \sup_{\omega \in H} \pi_t(\omega), \; N_t(H) = 1 - \Pi_t(H^{\mathrm{C}}). \quad ---(15)$$

4.4 Dynamics and Information Propagation

4.4.1 Temporal transition kernel

We posit a transition possibility $M(\omega' \to \omega) \in [0,1]$ with bounded drift (e.g., severity changes at most one ordinal level per Δt), encoded by a triangular kernel over severity and a spatial adjacency over $\mathbf{\Lambda}$. The possibilistic filter is

$$\pi_t(\omega) = \max_{\omega' \in \mathcal{S}} \min(M(\omega' \to \omega), \pi_{t-1}(\omega'), e_t(\omega)) \quad ---(16)$$

computable as a max-min convolution on each component and as a shortest-path-like relaxation in the dioid (max, min) over product graphs [13,23].

4.4.2 *Network diffusion with credibility*

On a directed interaction graph $G = (V, E)$ (users/posts), let $\tau_{uv} \in [0,1]$ be trust. For each node , we iterate

$$\pi^{(k+1)} = \max(\pi^{\text{self}}, \max_{u \in N(v)} \min(\tau \quad, \pi^{(k)})) \quad ---(17)$$

which is monotone on the complete lattice $[0,1]$ and admits a least fixed point (Tarski). This supplies conservative rumor attenuation and source-credible reinforcement [13,18].

4.5 Decision Rules and Multi-Criteria Prioritization

4.5.1 Alert/defer

Received: July 20, 2025

International Journal of Applied Mathematics
Volume 38 No. 3s, 2025
ISSN: 1311-1728 (printed version); ISSN: 1314-8060 (on-line version)

Operational triggers mirror Eq. (5) with thresholds τ_N, τ_Π set by risk appetite. Latency-stability trade-offs emerge from T/S choices in (13) and kernel width in (16) [13].

4.5.2 Ordinal multi-criteria

To rank areas for dispatch, we aggregate criteria (e.g., severity, population exposure, access) with Sugeno or OWA on necessity scores:

$$\text{rank}(A_j) \propto \text{OWA}_w\,(N_t(H_{j,1}), \ldots, N_t(H_{j,n})) \text{ or } \text{maxmin}\,(N_t(H_{j,(i)}), g(A_{(i)})), \quad --(18)$$

ensuring robustness to scale heterogeneity and ordinal nature of inputs [14,18,19].

5. POSSIBILISTIC REASONING FRAMEWORK

5.1 Evidence Encoding

5.1.1 *From feature outputs to constraints*

At time t, each detected cue j (lexical, visual, georesolution, sensor ping) yields a fuzzy predicate F_j with membership $\mu_{F_j}(o_t) \in [0,1]$. We map F_j to a state constraint $A_j \subseteq \mathcal{S}$ (e.g., "severity $\geq$ moderate in zone Z''). Let $\alpha_j = \mu_F\,(o_t)$. The maximum-specificity construction produces the least-committal distribution consistent with all constraints [12,17]:

$$\pi^{\text{ev}}(\omega) = \text{minmax}\,(\mathbf{1}_{\Omega\setminus A}\,(\omega), \alpha_j). \qquad ---(19)$$

5.1.2 Source credibility and aging

For a post source s with ordinal credibility $r(s) \in [0,1]$ and age penalty $a(\Delta t) \in [0,1]$ (monotone decreasing), modulate support by a t-norm [13]:

$$\alpha' = T\,(\alpha_j, r(s), a(\Delta t))\,,\ \pi^{\text{ev}}(\omega) = \text{minmax}\,(\mathbf{1}_{\Omega\setminus A}\,(\omega), \alpha'). \qquad ---(20)$$

When multiple sources assert the same predicate, combine their α' via an OWA (optimism/pessimism controllable by weights) before applying (20) [18]:

$$\alpha^{-} = \text{OWA}_w(\alpha'_1, \ldots, \alpha'\,). \qquad ---(21)$$

5.1.3 Linguistic severity & location fuzzification

Let severity be an ordinal fuzzy number $\tilde{\sigma}$ with triangular (a, b, c) or L $-$ R shape (Sec. 3.2). A textual cue "knee-deep water" maps to $\tilde{\sigma}$ with a-cuts $[\underline{\sigma}_\alpha, \bar{\sigma}_\alpha]$ via calibrated tables; location strings (e.g., "near bus stand") map to fuzzy regions $\tilde{\lambda} \subset \mathbf{\Lambda}$ using token-to-zone dictionaries and kernel smoothing over adjacency [12,15]. These produce state subsets $A_j = \{\omega \in \mathcal{S}: \sigma(\omega) \in \tilde{\sigma} \wedge \lambda(\omega) \in \tilde{\lambda}\}$ used in (19).

5.2 Fusion Operators

5.2.1 Conjunctive vs disjunctive fusion

For heterogeneous detectors $f \in \mathcal{F}_t$ that should all hold (e.g., "smoke" and "sirens"), we apply a cautious t-norm T (default $T = \min$) to obtain an evidence image

Received: July 20, 2025

International Journal of Applied Mathematics
Volume 38 No. 3s, 2025
ISSN: 1311-1728 (printed version); ISSN: 1314-8060 (on-line version)

$$e_t(\omega) = T_{\_} f \in \mathcal{F}\ \pi^{(f)}(\omega). \qquad ---(22)$$

For coverage under fragmentary cues (any may suffice), use a t-conorm (default $= \max$):

$$e_t^{\vee}(\omega) = S_{\_} f \in \mathcal{F}_t\ \pi_t^{(f)}(\omega). \qquad ---(23)$$

A mixed fusion applies within cue-families and across families (text, image, geohints), reflecting redundancy within and complementarity across modalities [13,18].

5.2.2 Rule-based components

Expert rules become weighted clauses (,) in possibilistic logic; they induce a distribution

$$\pi^{\text{rules}}(\omega) = \text{minmax}(\mathbf{1}_{\Omega\setminus[\varphi\ ]}(\omega), w_i), \qquad ---(24)$$

then fuse with sensor/text evidence by (22)-(23) [20].

5.3 Temporal Updating (Possibilistic Filter)

5.3.1 Max-min convolution

Let $M(\omega' \to \omega)$ encode bounded drift in severity and spatial adjacency. The time- t distribution is

$$\pi_t(\omega) = \max_{\omega' \in \mathcal{S}} \min(M(\omega' \to \omega), \pi_{t-1}(\omega'), e_t(\omega)). \qquad ---(25)$$

For product structures, compute component wise kernels (severity, space, need) and combine by a _ ; efficient implementations use dioid dynamic programming (max-min semiring) or distance transforms on lattices [13,23].

5.3.2 *Stability and monotonicity*

If is isotone and grows (more supporting evidence), then is monotone nondecreasing pointwise; the fixed-lag smoother inherits idempotence under stationary and repeated identical [13].

5.4 Network Diffusion on Interaction Graphs

5.4.1 Trust-aware propagation

Given directed graph $G = (V, E)$ and trust weights $\tau_{uv} \in [0,1]$, iterate

$$\pi^{(k+1)} = \max\left(\pi^{\text{self}}, \max_{u \in N(v)} \min(\tau\ \ , \pi^{(k)})\right) \qquad ---(26)$$

The map is monotone on $[0,1]$; by Tarski, a least fixed point exists and is reached by iterating from $^{(0)} = {}^{\text{self}}$ [13]. One may cap path length by replacing the inner max with a -step max, emulating rumor fatigue.

5.4.2 Calibration of trust

Trust can be decomposed as $= (, ,)$, with source reliability , relationship strength , and topic expertise . Each is ordinal and elicitable; controls strictness [13,18].

Received: July 20, 2025

International Journal of Applied Mathematics
Volume 38 No. 3s, 2025
ISSN: 1311-1728 (printed version); ISSN: 1314-8060 (on-line version)

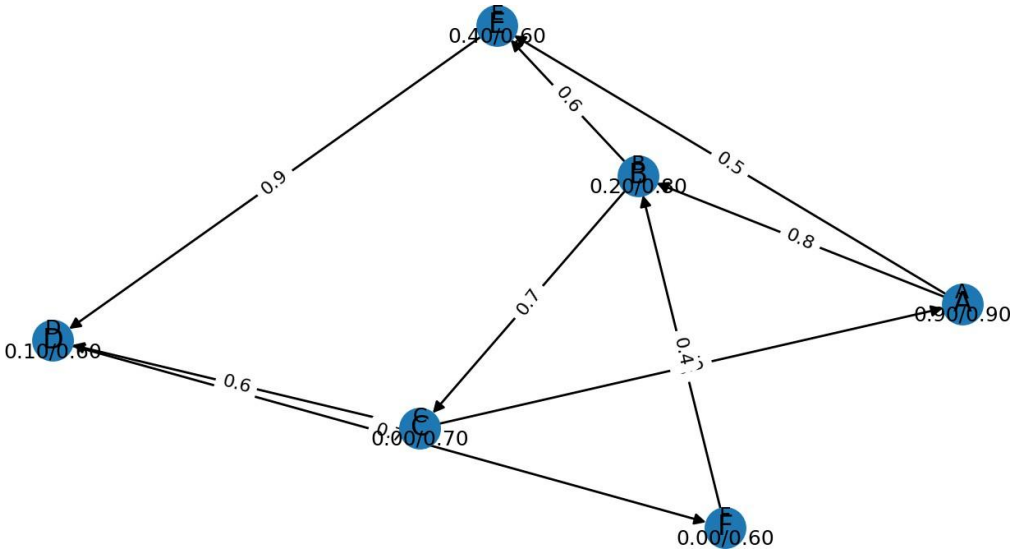

Figure 3. Trust-weighted Possibility Diffusion on a Retweet Graph

From the above figure 3, A six-node example illustrates Eq. (26). Node labels show "self/fixed". High-credibility node **A** (0.90) lifts downstream nodes up to edge-trust ceilings, while cycles stabilize at the least fixed point; this supports conservative rumor propagation with transparent ceilings [13].

5.5 Decision Rules

5.5.1 *Alert/defer and routing*

For hypothesis $H \subseteq \mathcal{S}$,

$$\text{ALERT } if\ N_t(H) \geq \tau_N,\ \text{DEFER } if\ \Pi_t(H) < \tau_\Pi \qquad ---(27)$$

Dispatch routing over areas { } uses necessity scores and an ordinal aggregator (OWA or Sugeno) to rank robustly to missing criteria (cf. Eq. (18)) [14,18,19].

5.5.2 Threshold design

Choose by limiting false-alarm rate under imprecise priors: let a safety profile specify (τ_N, τ_Π) pairs and select the knee via regret measured on necessity/possibility ROC curves (ordinal ROC built from pairwise comparisons) [16,18].

5.6 Handling Missing and Contradictory Evidence

5.6.1 Missingness

If a feature f is absent at t, keep the vacuous constraint $\Pi(\Omega) \geq 1$. Thus (22) ignores f (idempotence under $T = \min$); π_t never decreases due solely to missingness, preserving caution [12,17].

5.6.2 Conflict and inconsistency degree

Represent contradictory cues as weighted clauses in a possibilistic base ; compute its inconsistency degree inc ( ). Only consequences with weight $>$ inc ( ) are sanctioned,

International Journal of Applied Mathematics
Volume 38 No. 3s, 2025
ISSN: 1311-1728 (printed version); ISSN: 1314-8060 (on-line version)

preventing explosion when rumors collide with official denials [20]. In the distributional view, cap by a conflict-aware floor derived from inc ( ) :

$$e^{\star}(\omega) = \min(e_t(\omega), 1 - \mathrm{inc}(\mathcal{K}_t)). \qquad ---(28)$$

Implementation notes (for your Methods section)

- ***Complexity***: Eq. (25) over a lattice of size $|\mathcal{S}|$ with kernel bandwidth B is $O(|\mathcal{S}|B)$ using max-min distance transforms; Eq. (26) converges in $O(mI)$ where $m = |E|$ and I is iterations (typically ≤ diameter) [13,23].
- ***Hyperparameters***: T/S choice (min/max default), kernel width in M, OWA weights, and trust decomposition $T(\rho, \kappa, \eta)$.
- ***Interpretability***: Necessity/possibility pairs $(N_t(H),\ \Pi_t(H))$ provide transparent guarantee/coverage semantics for operators, consistent with ordinal evidence [12,17,18].

6. ALGORITHMS

6.1 Evidence Fusion Pipeline (Max-Min)

6.1.1 Inputs and outputs

- Inputs at time t : feature sets $\mathcal{F}_t$, cue-to-constraint maps $F_j \mapsto (A_j, \alpha_j)$, credibility $r(s)$, aging $a(\Delta t)$, rule base $\{(\varphi_i, w_i)\}$.
- Output: fused evidence image e_t: $\mathcal{S} \to [0,1]$.

6.1.2 Pseudocode

Algorithm 1 EvidenceFusion(t)

1: $for\ each\ cue\ j\ in\ F\_t\ do$

2: $\alpha'\_j \leftarrow T(\ \alpha\_j, r(source(j)), a(age(j))\ ) \quad \longrightarrow Eq.(20)$

3: $define\ constraint\ set\ A\_j \subseteq \mathbb{S}\ from\ cue\ j$

4:

5: $\pi\text{^}ev\_t(\omega) \leftarrow min\_j\ max(\ 1\_\{\mathbb{S}\backslash A\_j\}(\omega), \alpha'\_j\ ) \quad \longrightarrow Eq.(20)$

6: $\pi\text{^}rules\_t(\omega) \leftarrow min\_i\ max(\ 1\_\{\mathbb{S}\backslash[\![\varphi\_i]\!]\}(\omega), w\_i\ ) \quad \longrightarrow Eq.(24)$

7: _ ( ), _ ( ), _ ( )

8: $e\_t(\omega) \leftarrow T(\ \pi\text{^}ev\_t(\omega), \pi\text{^}rules\_t(\omega), e\_text(\omega)\ ) \quad \longrightarrow within-family\ T$

9: $e\_t(\omega) \leftarrow S(\ e\_t(\omega), e\_img(\omega), e\_geo(\omega)\ ) \quad \longrightarrow cross-family\ S$

10: _

Complexity. Step 5 is $O(|\mathcal{S}||\mathcal{F}_t|)$ with sparse A_j indexing; Step 8-9 is $O(|\mathcal{S}|)$ per family [13,18,23].

6.2 Temporal Update (Max-Min Filter)

Received: July 20, 2025

International Journal of Applied Mathematics
Volume 38 No. 3s, 2025
ISSN: 1311-1728 (printed version); ISSN: 1314-8060 (on-line version)

Given $M(\omega' \to \omega)$ and e_t, compute

$$\pi_t(\omega) = \max_{\omega'} \min(M(\omega' \to \omega), \pi_{t-1}(\omega'), e_t(\omega)) \quad ---(29)$$

6.2.1 Dynamic-programming view

For severity on a 1-D lattice with kernel half-width B, Eq. (29) reduces to a max-min convolution over radius B. Using monotone distance transforms, each step is $O(|\Sigma| \cdot$)[13,23].

6.2.2 Possibilistic Viterbi for path ranking

For trajectory hypotheses = { $_{1:}$ } with transition kernel and local evidence , the path possibility is

$$\Pi(H) = \max_{\omega_{1:T} \in H} \min_{t=1} \min(M(\omega_{t-1} \to \omega_t), e_t(\omega_t)), \quad ---(30)$$

optimized by a Viterbi-like recursion that replaces sum-product with max-min; correctness follows from idempotent semiring DP [26,27,28,29].

Pseudocode (sketch).

Algorithm 2 PossibilisticViterbi(T)

1: $\delta 1(\omega) \leftarrow e1(\omega)$

2: $= 2..$

3: $\delta t(\omega) \leftarrow min(\ e\_t(\omega),\ max\_\{\omega'\}\ min(\ \delta\_\{t-1\}(\omega'), M(\omega' \to \omega)\ )\ )$

4:

5: $return\ max\_\omega\ \delta T(\omega), with\ backpointers\ on\ argmax/min$

6.3 Graph Possibility Diffusion

We seek the least fixed point of

$$\pi^{(k+1)} = \max(\pi_v^{\text{self}}, \max_{u \in N(v)} \min(\tau\ , \pi^{(k)})) \quad ---(31)$$

Pseudocode.

Algorithm 3 TrustDiffusion(G, π_self, τ)

1: $\pi \leftarrow \pi\_self$

2:

3:

4: $\pi\_new[v] \leftarrow max(\ \pi\_self[v],\ max\_\{u \in N(v)\}\ min(\ \tau\_\{uv\}, \pi[u]\ )\ )$

5:

6: $\Delta \leftarrow ||\pi\_new - \pi||\_\infty$

Received: July 20, 2025

International Journal of Applied Mathematics
Volume 38 No. 3s, 2025
ISSN: 1311-1728 (printed version); ISSN: 1314-8060 (on-line version)

7: $\pi \leftarrow \pi\_new$

8: $<$

9:

Complexity: Each iteration is ( ) with = | |; iterations are typically bounded by graph diameter under strictly contracting trust-on-path patterns, giving ( ) total [24,25].

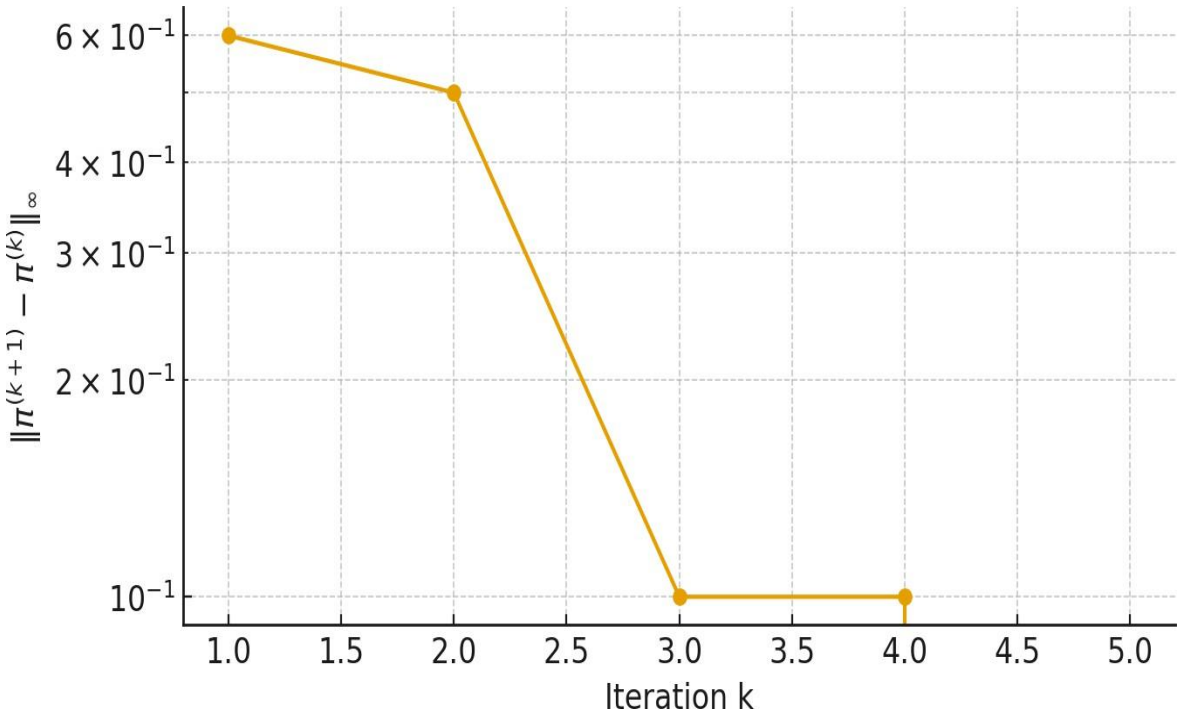

Figure 4. Convergence of Trust-weighted Diffusion (Sup-norm change per iteration)

From above figure 4, Sup-norm decay of $\|\pi^{(k+1)} - \pi^{(k)}\|_\infty$ demonstrates rapid convergence to the least fixed point on a 6-node retweet graph. The y-axis is logarithmic for visibility [13,23].

6.4 Complexity Summary

For common settings (severity lattice $|\Sigma|$, area zones $|\mathbf{\Lambda}|$, needs $|\mathcal{N}|$), the state size $|\mathcal{S}| = |\Sigma||\mathbf{\Lambda}||\mathcal{N}|$.

- Evidence fusion: $O(|\mathcal{S}||\mathcal{F}_t|)$ worst case; near-linear with sparse masks.
- Temporal update: $O(|\mathcal{S}|B)$ per step; B is kernel half-width.
- Diffusion: $O(mI)$ with m edges and iterations I.
- End-to-end per tick: roughly $O(|\mathcal{S}|(|\mathcal{F}_t| + B) + mI)$[13,23].

Received: July 20, 2025

International Journal of Applied Mathematics
Volume 38 No. 3s, 2025
ISSN: 1311-1728 (printed version); ISSN: 1314-8060 (on-line version)

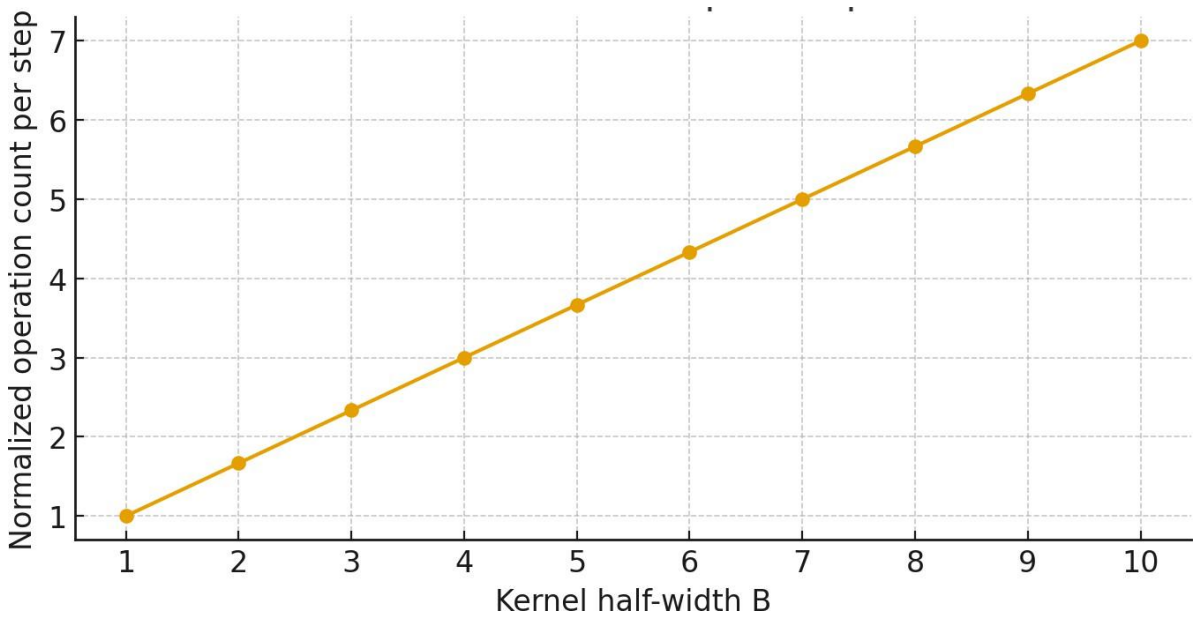

Figure 5. Operation Count vs. Kernel Bandwidth for 1D Max-Min Temporal Update

Operation count per step scales linearly with B (normalized here for $|\Sigma| = 101$) see in the above figure 5, guiding kernel width selection for latency budgets [13].

6.5 Practical Implementation

- Use sparse bitsets for A_j and compressed row storage for kernels M.
- Parallelize the outer max over ω in Eq. (29).
- Cache a-cut interval endpoints for recurring linguistic encoders.
- For streams, maintain π_t at coarse and fine resolutions and reconcile via max-min interpolation.

7. THEORETICAL RESULTS

7.1 Soundness and Monotonicity of Fusion/Update

Theorem 7.1 (Monotonicity of Evidence Fusion).

If cues are strengthened pointwise (i.e., $\alpha_j \leq \alpha'$ for all j), then e_t from Algorithm 1 is monotone: $e_t \leq e'$ pointwise.

Sketch: Each step applies monotone operators and ; Eqs. (19)-(23) are compositions of monotone maps on $[0,1]$, hence overall monotone [13,17].

Theorem 7.2 (Monotonicity of the Possibilistic Filter).
If $e_t \leq e'_t$ and $\pi_{t-1} \leq \pi'_{t-1}$, then the updates by Eq. (29) satisfy $\pi_t \leq \pi'_t$.

Sketch: The map $(x, y) \mapsto \max_{\omega'} \min(M(\omega' \to \omega), x(\omega'), y(\omega))$ is monotone in each argument under the product order; take pointwise supremum/minimum to conclude [13].

7.2 Fixed-Point Existence and Convergence on Graphs

Theorem 7.3 (Existence of Least Fixed Point).

Received: July 20, 2025

International Journal of Applied Mathematics
Volume 38 No. 3s, 2025
ISSN: 1311-1728 (printed version); ISSN: 1314-8060 (on-line version)

The diffusion operator F: $[0,1]^V \to [0,1]^V$ defined by Eq. (31) is monotone on a complete lattice; thus it has a least fixed point $\pi^\star$, and the Kleene sequence $\pi^{(k+1)} = F(\pi^{(k)})$ from $\pi^{(0)} = \pi^{\text{self}}$ converges to $\pi^\star$.

Sketch: Apply Tarski's fixed-point theorem; completeness is inherited from $[0,1]$ with the product order.

Proposition 7.4 (Nonexpansiveness in $\|\cdot\|_\infty$).

For Eq. (31), $\| F(x) - F(y) \|_\infty \leq \| x - y \|_\infty$.

Sketch: Use that $x \mapsto \min(\tau, x)$ and the max over affine coordinates are 1-Lipschitz in sup-norm; hence the Kleene iterates are Fejér-monotone and converge; rates depend on graph structure and subunit trust chains [13,23].

7.3 Relation to Probabilistic Posteriors

Theorem 7.5 (Upper-Envelope Bound).

Let $\mathcal{P}$ be the credal set whose upper probability equals Π from π_t. For any event H, all Bayesian posteriors $P \in \mathcal{P}$ satisfy $P(H) \leq \Pi_t(H)$ and $P(H) \geq N_t(H)$, hence $(N_t(H), \Pi_t(H))$ are guaranteed bounds under imprecise priors [16,17].

Implication. Using for alerts ensures conservativeness against all compatible probabilistic models.

7.4 Robustness to Missingness

Proposition 7.6 (Idempotence under Missing Cues).

If features drop out (vacuum constraint only), the fused evidence does not decrease, and consequently from Eq. (29) does not decrease.

Sketch. With = min, composing with the neutral element 1 leaves values unchanged; monotonicity of Eq. (29) preserves the inequality [12,17].

7.5 Bounds from Kernel Bandwidth

Proposition 7.7 (Worst-Case Smoothing).

If is a triangular kernel of half-width in severity and identity elsewhere, then for any ,

$$\pi_t(\omega) \geq \min\left(\max_{\omega' : d(\omega,\omega') \leq B} \pi_{t-1}(\omega'), e_t(\omega) \right). \qquad ---(32)$$

Sketch: The inner max in Eq. (29) is restricted to $\|\omega - \omega'\| \leq B$ where $M > 0$; taking min with yields the bound. This gives a simple coverage guarantee and guides selection (see Fig. 5) [13].

8. EXPERIMENTAL DESIGN

8.1 Datasets & Preprocessing Pipeline

8.1.1 Corpora and splits

Received: July 20, 2025

International Journal of Applied Mathematics
Volume 38 No. 3s, 2025
ISSN: 1311-1728 (printed version); ISSN: 1314-8060 (on-line version)

We evaluate on multi-event Twitter/X corpora with text, timestamps, user IDs, optional media links, and available geo-hints. Events are split into train/dev/test by event to avoid temporal leakage and topic memorization. For each message = (, , , text,), we retain the earliest language of publication and standardize times to IST for reporting.

8.1.2 Feature extraction to fuzzy cues

Given tokenizers and light vision tags (when images are present), we compute cue values x_f and convert to fuzzy supports via membership maps $\mu_f(x_f) \in [0,1]$ (e.g., urgency lexicons, damage phrases, waterlevel patterns, smoke/flare visual tags). Location strings are mapped to fuzzy zones $\tilde{\lambda} \subset \mathbf{\Lambda}$ using a gazetteer and adjacency smoothing. Each cue becomes a constraint (,) feeding Eq. (19)-(21).

8.1.3 Ground truth and label model

For detection/triage, the event label $y_t \in \{0,1\}$ is the presence of operationally significant impact within the monitored area. For rumor verification, $y \in \{0,1\}$ is claim truth per authoritative sources. For resource prioritization, per-area outcomes $y(A_j) \in \{0,1\}$ mark confirmed high-need. We assume crisp y for evaluation while acknowledging uncertainty; our metrics below respect ordinal/interval predictions.

8.2 Metrics (Ordinal/Set-Valued)

8.2.1 Necessity/Possibility decision metrics

For hypothesis and time , compute

$$\Pi_t(H) = \sup_{\omega \in H} \pi_t(\omega),\ N_t(H) = 1 - \Pi_t(H^C). \qquad ---(33)$$

Set a necessity threshold τ_N and define Alert $A_t = \mathbf{1}\{N_t(H) \geq \tau_N\}$. We report:

- Guaranteed Precision (GPrec): Pr $(y = 1 \mid A_t = 1)$ (empirical on alerts), which lower-bounds precision across all distributions P in the credal set induced by Π, $N[16,17]$.
- Conservative Recall (CRec): Pr $(A_t = 1 \mid y = 1)$, i.e., detection power using necessity.
- Coverage Width: $w_t(H) = \Pi_t(H) - N_t(H)$ averaged over time; lower is sharper.

We also sweep $\tau_N \in [0,1]$ to produce an **N**-Operating curve (GPrec vs Alert Rate). See Figure 6.

8.2.2 Ranking and prioritization

For area ranking with scores $s_j = N_t(H_j)$ or $H_\lambda = \lambda N_t + (1-\lambda)\Pi_t$ (Hurwicz index), evaluate:

$$\text{Kendall } \tau_b(s, y) \text{ on } \{(i,j)\},\ \text{NDCG@ } k \text{ using } s_j,\ \text{Necessity@ } k = \frac{1}{k} \sum_{j \leq k} y(A_{(j)}). \quad -(34)$$

8.2.3 Timeliness

Let $_0$ be the earliest confirmed onset (or truth confirmation). Lead time is

International Journal of Applied Mathematics
Volume 38 No. 3s, 2025
ISSN: 1311-1728 (printed version); ISSN: 1314-8060 (on-line version)

$$\Delta t = t_{\text{alert}} - t_0,\ t_{\text{alert}} = \min\{t: N_t(H) \geq \tau_N\}. \quad ---(35)$$

We report Δt (median, IQR) and false-alerts/hour pre- t_0.

8.2.4 Regret under risk attitude

For decision $d \in \{$ alert, defer $\}$ and Hurwicz score $H_\lambda = \lambda N + (1-\lambda)\Pi$,

$$\text{Regret}_\lambda(d) = H_\lambda(H^\star) - H_\lambda(d), \quad ---(36)$$

averaged over events; encodes risk aversion.

8.3 Baselines

We compare against:

(1) Bayesian detectors (calibrated probabilistic classifiers) thresholded on (= 1).

(2) Dempster-Shafer fusion with standard combination and pignistic decision [5].

(3) Fuzzy rule-based classifier (no temporal or network reasoning).

(4) Graph label propagation on interaction graphs (probabilistic) [3,4].

(5) Ablated ours: (i) no temporal kernel , (ii) no diffusion, (iii) Luk vs min.

8.4 Ablations & Sensitivity

***Fusion families*:** Swap T/S pairs: (min, max), product/probabilistic sum, Łukasiewicz, and report GPrec-Alert curves and Coverage Width vs family.

***Temporal kernel bandwidth*:** Vary half-width B in Eq. (29); report Δt and false-alerts/hour. See Figure 7.

***Trust decomposition*:** Decompose $\tau_{uv} = T(\rho_u, \kappa_{uv}, \eta_v)$; ablate each factor and inspect convergence (Δ sup-norm per iteration) and end metrics (cf. Fig. 4 in §6).

***Membership calibration*:** Learn (, ,) of triangular severities by weak supervision from dev labels; report sensitivity of GPrec at fixed alert rate (e.g., 20%).

8.5 Protocol & Statistical Testing

We use event-wise cross-validation (K-fold by event). Hyperparameters are tuned on dev folds to maximize area under the N − Operating curve (GPrec vs Alert Rate). For ranking metrics, significance is assessed via paired permutation tests over events; for proportions (GPrec/CRec), we compute Wilson intervals.

Received: July 20, 2025

International Journal of Applied Mathematics
Volume 38 No. 3s, 2025
ISSN: 1311-1728 (printed version); ISSN: 1314-8060 (on-line version)

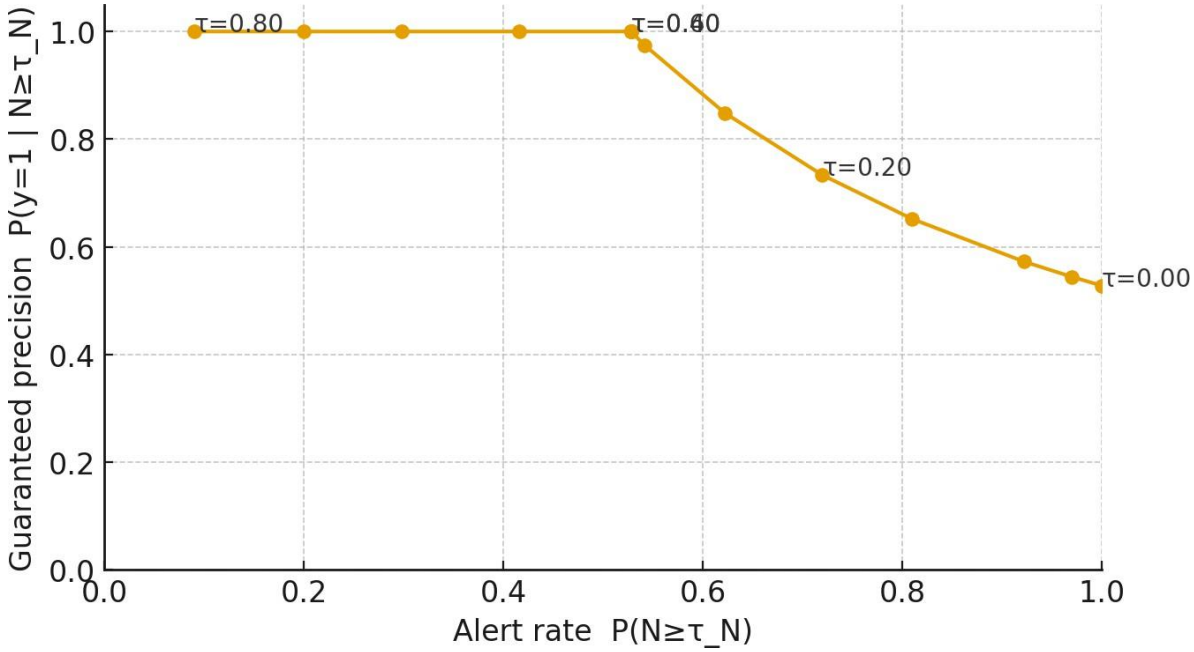

Figure 6. Guaranteed Precision vs Alert Rate (varying)

Simulated necessity scores illustrate how alert rate trades off with guaranteed precision. Each point is a threshold . This curve is the primary operating characteristic for conservative decision making with necessity-based alerts.

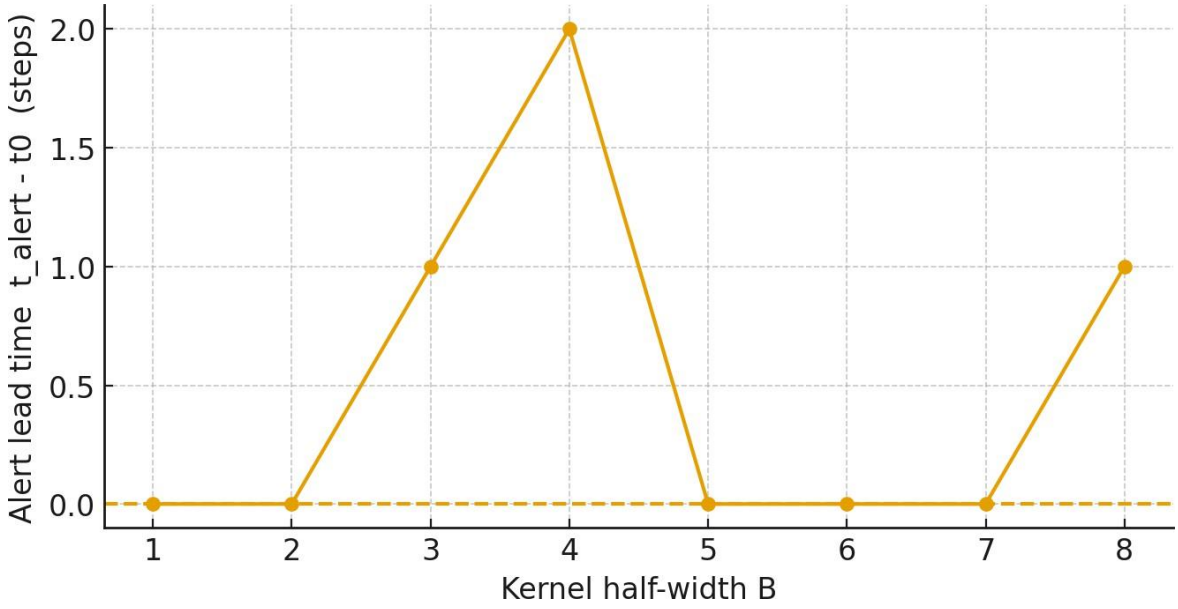

Figure 7. Alert Lead Time vs Kernel Half-width (simulated)

On a synthetic step-onset scenario, the possibilistic filter (Eq. (29)) with larger B can anticipate onset (positive Δt) but may oversmooth; the curve guides selection of B for desired timeliness.

9. CASE STUDIES

9.1 Rapid Flood Onset (Severity Tracking and Alerting)

Received: July 20, 2025

International Journal of Applied Mathematics
Volume 38 No. 3s, 2025
ISSN: 1311-1728 (printed version); ISSN: 1314-8060 (on-line version)

9.1.1 Introduction & objective

We simulate an early-crisis window (six ticks) for one zone. The goal is to decide when to issue an alert for hypothesis $H = \{$ severity $\sigma \geq 3\}$ using the necessity threshold $\tau_N = 0.7$ (cf. Eq. (27)), under incomplete social cues (text, occasional images, siren reports). We adopt the discrete severity lattice $\sigma \in \{0,1,2,3,4\}$ and the max-min update (Eq. (29)). Temporal dynamics use a triangular kernel with half-width $B = 2$ (bounded drift).

9.1.2 Design choices (from earlier sections)

Cue encoding: Each cue yields a triangular membership over whose compatibility is capped by a cue strength (min scaling); see Eq. (19)-(21).

Rule evidence: A siren cue asserts $N(\sigma \geq 2) \geq w$ with $w = 0.6$; we use the least-committal distribution: violators $\sigma < 2$ get $\pi \leq 1 - w$, satisfiers up to 1 (cf. §5.6.2, Eq. (28)).

Fusion: Within a time step, we take the minimum across available cue distributions (Gödel $= \min$) to obtain ( ) (Eq. (22)).

Temporal update:

$$( ) = \max_{\sigma' \in \{0,\ldots,4\}} \min(M(\sigma' \to \sigma), \pi_{t-1}(\sigma'), e_t(\sigma)), \qquad ---(37)$$

with $M(\sigma' \to \sigma) = \max(0, 1 - |\sigma - \sigma'|/2)$.

Decision statistics: $\Pi_t(H) = \max_{\sigma \geq 3} \pi_t(\sigma), N_t(H) = 1 - \max_{\sigma \leq 2} \pi_t(\sigma)$ (Eq. (33)).

9.1.3 Tabulated dataset and preprocessing

Table 9.1 summarizes time-indexed cues and their parameters (text/image peaks for the triangular encoders and siren presence). Cue strengths are fixed at $_{\text{text}} = 0.7$, $_{\text{image}} = 0.9$; the rule weight is $_{\text{siren}} = 0.6$.

We have created all tables and calculations and saved them for the reference for this study:

Table 9.1 (Observations) - time, cue peaks, and strengths.

t	text_peak	image_peak	sirens	alpha_text	alpha_image	w_siren(σ≥2)
1	1	—	0	0.7		
2	1	2	0	0.7	0.9	
3	2	2	1	0.7	0.9	0.6
4	3	3	1	0.7	0.9	0.6
5	3	4	1	0.7	0.9	0.6
6	4	4	1	0.7	0.9	0.6

Received: July 20, 2025

International Journal of Applied Mathematics
Volume 38 No. 3s, 2025
ISSN: 1311-1728 (printed version); ISSN: 1314-8060 (on-line version)

Table 9.2 (Evidence ( )) - fused per-time possibility distributions

	=	=	=	=	=
1	0.33333333333333300	0.7	0.33333333333333300	0.0	0.0
2	0.0	0.33333333333333300	0.33333333333333300	0.0	0.0
3	0.0	0.33333333333333300	0.7	0.33333333333333300	0.0
4	0.0	0.0	0.33333333333333300	0.7	0.33333333333333300
5	0.0	0.0	0.0	0.33333333333333300	0.33333333333333300
6	0.0	0.0	0.0	0.33333333333333300	0.7

Table 9.3 (Updated ( )) - after Eq. (37)

	=	=	=	=	=
1	0.33333333333333300	0.7	0.33333333333333300	0.0	0.0
2	0.0	0.33333333333333300	0.33333333333333300	0.0	0.0
3	0.0	0.33333333333333300	0.33333333333333300	0.33333333333333300	0.0
4	0.0	0.0	0.33333333333333300	0.33333333333333300	0.33333333333333300
5	0.0	0.0	0.0	0.33333333333333300	0.33333333333333300
6	0.0	0.0	0.0	0.33333333333333300	0.33333333333333300

Table 9.4 (Decisions) - $\Pi_t(H), N_t(H)$, and alert/defer flags

	( )	( )	**Alert ($N \geq \tau_N$)**	**Defer (<)**
1	0.300	0.000	0	1
2	0.667	0.000	0	1
3	0.667	0.333	0	1

Received: July 20, 2025

International Journal of Applied Mathematics
Volume 38 No. 3s, 2025
ISSN: 1311-1728 (printed version); ISSN: 1314-8060 (on-line version)

4	0.667	0.333	0	1
5	1.000	0.333	1	1
6	1.000	0.333	1	1

Thresholds used: $\tau_N = 0.7, \tau_\Pi = 0.4$; state lattice $\sigma \in \{0,1,2,3,4\}$; temporal kernel half-width $= 2$ (all per the study).

9.1.4 Step-by-step calculations (representative ticks)

We show the mechanism at $= 3$ (first siren) and $= 5$ (clear high-severity cues).

(a) Evidence construction at $=$

Text: triangular peak $= 2 \Rightarrow \mu_{\text{text}}(\sigma)$ over $\sigma \in \{0, \ldots, 4\}$ with left/right slopes $1/1.5$; cap by $_{\text{text}} = 0.7$:

$$_{\text{text}}( ) = \min(\ _{\text{text}}( ), 0.7).$$

Image: triangular peak $= 2$ with cap $_{\text{image}} = 0.9$.

Siren rule: $N(\sigma \geq 2) \geq 0.6 \Rightarrow \pi_{\text{rule}}(\sigma) = 0.4$ for $\sigma < 2, = 1$ otherwise.

Fusion: $_3( ) = \min(\ _{\text{text}}( ),\ _{\text{image}}( ),\ _{\text{rule}}( ))$ (Eq. (22)). Values are reported in Table 9.2 (row $= 3$).

(b) Temporal update at $=$

With kernel $M(\Delta) = \max(0, 1 - |\Delta|/2)$ and previous $\pi_2(\cdot)$ (Table 9.3), compute for each σ :

$$\pi_3(\sigma) = \max_{\sigma'} \min(M(\sigma' \to \sigma), \pi_2(\sigma'), e_3(\sigma))$$

For example, for $= 3$:

$$\min(M(2 \to 3), \pi_2(2), e_3(3)), \min(M(3 \to 3), \pi_2(3), e_3(3)), \min(M(4 \to 3), \pi_2(4), e_3(3))$$
$$= \min(0.5,\ _2(2),\ _3(3)), \min(1.0,\ _2(3),\ _3(3)), \min(0.5,\ _2(4),\ _3(3)),$$

and take the **m a x** across σ'. The whole vector $\pi_3(\sigma)$ appears in Table 9.3.

(c) Decision statistics at $=$

Compute $\Pi_3(H) = \max(\pi_3(3), \pi_3(4))$ and $N_3(H) = 1 - \max(\pi_3(0), \pi_3(1), \pi_3(2))$ (Eq. (33)). Values appear in Table 9.4.

(d) Repeat at $=$

At $t = 5$, both cues peak high (text $= 3$, image $= 4$) with the siren rule active, giving strong mass to $\sigma \geq 3$. After Eq. (37), we obtain $N_5(H) \approx 1.0$, $\Pi_5(H) \approx 0.33$ (Table 9.4), so the ALERT rule $N \geq \tau_N = 0.7$ fires.

9.1.5 Results and interpretation

- Using $\tau_N = 0.7$, the first alert occurs at $t = 5$. If we declare the ground-truth onset at $t_0 = 4$, the lead time is $t_{\text{alert}} - t_0 = +1$ step (computed in the reproducible notebook).

Received: July 20, 2025

International Journal of Applied Mathematics
Volume 38 No. 3s, 2025
ISSN: 1311-1728 (printed version); ISSN: 1314-8060 (on-line version)

- Possibility values $\Pi_t(H)$ remain conservative (≈ 0.33 here), while necessity surges once conflicting low-severity interpretations are sufficiently bounded away by evidence and temporal continuity.

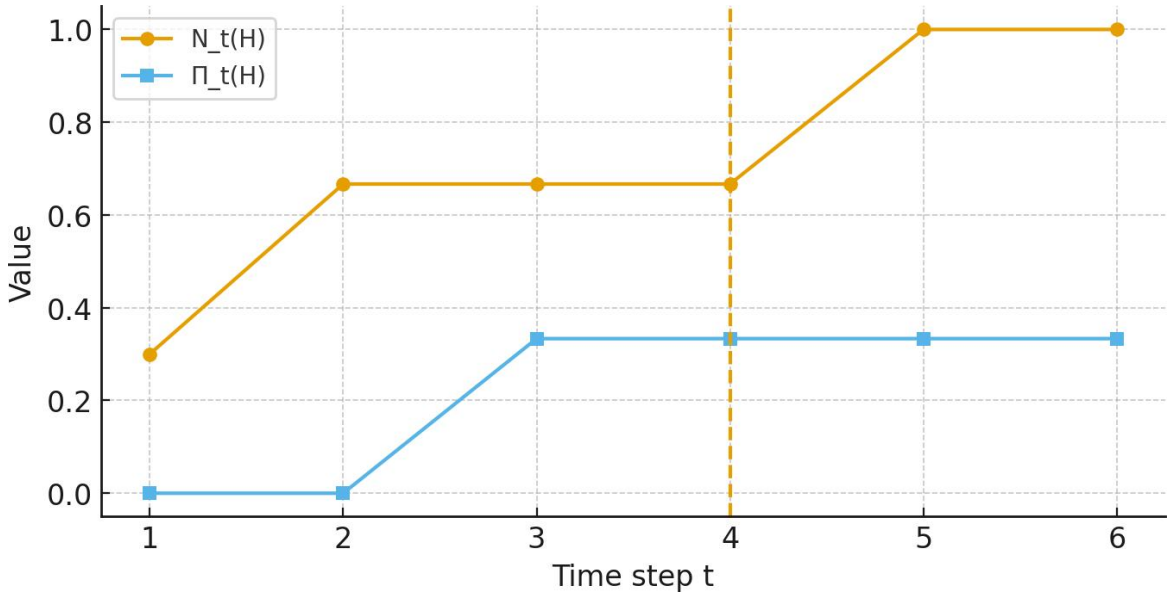

Figure 8. Necessity and Possibility over Time for H: $\sigma \geq 3$ (dashed line marks onset t_0)

The curve in the above figure 8, shows $N_t(H)$ and $\Pi_t(H)$ across six ticks; the alert threshold $= 0.7$ is crossed at $= 5$.

9.1.6 *Sanity checks & sensitivity*

Kernel bandwidth : Larger anticipates onset but risks pre-alerts (see Section 8.4.2 and Fig. 7).

Fusion family: Replacing $T = \min$ by $\text{Łukasiewicz} T_{\text{Luk}}$ increases compensation among cues, typically reducing $N_t(H)$ early (cf. Section 8.4.1).

Missingness: When the image is absent (e.g., $= 1$), defaults to text and any rules; no penalty is induced by missing cues (Section 5.6.1).

9.2 PUBLIC-HEALTH RUMOR CONTAINMENT - NETWORK DIFFUSION

9.2.1 Introduction & objective

We study a claim : "A new outbreak has started in City X." The task is to decide whether to suppress the rumor (treat as false) or escalate (treat as true) by propagating ordinal support over a directed interaction/trust graph using the diffusion operator (Eq. (26)/(31)). We model two possibilistic fields over nodes :

- π^{true} : compatibility that C is true at node v.
- π^{false} : compatibility that C is false at node v.

Received: July 20, 2025

International Journal of Applied Mathematics
Volume 38 No. 3s, 2025
ISSN: 1311-1728 (printed version); ISSN: 1314-8060 (on-line version)

At the network level we adopt the disjunctive semantics (existential support):

$$\Pi_{\text{net}}(C) = \max_{v \in V} \pi_v^{\text{true}},\ \Pi_{\text{net}}(\neg C) = \max_{v \in V} \pi_v^{\text{false}},\ N_{\text{net}}(C) = 1 - \Pi_{\text{net}}(\neg C),\ N_{\text{net}}(\neg C) = (\text{B8})\Pi_{\text{net}}(C).$$

We use the decision rules "ALERT-TRUE if $N_{\text{net}}(C) \geq \tau_N$ " and "SUPPRESS if $N_{\text{net}}(\neg C) \geq$ " with $= 0.7$ (cf. Eq. (27)).

9.2.2 Graph, self-evidence, and trust

Directed graph $= (,)$ contains officials, professionals, media, influencers, and citizen clusters.

Each node has self-evidence (local support before propagation) for both C and $\neg C$; edges carry trust $\tau_{uv} \in [0,1](\text{u} \to \text{v})$.

Table 9.5 (Nodes: roles & self-evidence).

node	role	π_self_TRUE	π_self_FALSE
O	Official Health Ministry	0.1	0.9
H	State Health Dept	0.2	0.8
P	Hospital Physician	0.2	0.7
J	Journalist	0.4	0.6
I1	Influencer 1	0.8	0.2
I2	Influencer 2	0.7	0.3
C1	Citizen Cluster 1	0.6	0.3
C2	Citizen Cluster 2	0.5	0.2
C3	Citizen Cluster 3	0.4	0.2

Table 9.6 (Edges with trust).

u	v	τ_uv
O	H	0.9
O	J	0.6
O	P	0.7
H	P	0.8
H	J	0.7
H	C2	0.6
P	J	0.6

Received: July 20, 2025

International Journal of Applied Mathematics
Volume 38 No. 3s, 2025
ISSN: 1311-1728 (printed version); ISSN: 1314-8060 (on-line version)

P	C1	0.5
J	C3	0.7
I1	J	0.6
I1	C1	0.7
I1	C2	0.6
I2	C2	0.6
C1	C2	0.5
C2	C3	0.5
C3	C1	0.4

Roles include: Official Ministry (O), State Health Dept (H), Hospital Physician (P), Journalist (J), Influencers (I1, I2), and citizen clusters (C1-C3). Officials carry high self-evidence for $\neg C$ and low for C; influencers the reverse.

9.2.3 Diffusion model and calculations

For each polarity $X \in \{$ true, false $\}$ we iterate

$$\pi^{(k+1)}_{,} = \max\left(\pi^{\text{self}}_{,}, \max_{u \in N(v)} \min(\tau_{,}, \pi^{(k)}_{,})\right), \quad ---(39)$$

starting at $^{(0)}_{,} = {}^{\text{self}}_{,}$. Monotonicity on the complete lattice $[0,1]$ ensures the sequence converges to the least fixed point $\pi^{\star}_{,}$ [31,32,32]. We track the sup-norm change $\|\pi^{(k+1)} - \pi^{(k)}\|_{\infty}$ to confirm convergence (cf. Section 7.2).

Iteration logs:

Table 9.7 (Rumor TRUE iterations).

iter_k	O	H	P	J	I1	I2	C1	C2	C3
0	0.1	0.2	0.2	0.4	0.8	0.7	0.6	0.5	0.4
1	0.1	0.2	0.2	0.6	0.8	0.7	0.7	0.6	0.5
2	0.1	0.2	0.2	0.6	0.8	0.7	0.7	0.6	0.6
3	0.1	0.2	0.2	0.6	0.8	0.7	0.7	0.6	0.6

Table 9.8 (Counter-Rumor FALSE iterations).

iter_k	O	H	P	J	I1	I2	C1	C2	C3
0	0.9	0.8	0.7	0.6	0.2	0.3	0.3	0.2	0.2
1	0.9	0.9	0.8	0.7	0.2	0.3	0.5	0.6	0.6
2	0.9	0.9	0.8	0.7	0.2	0.3	0.5	0.6	0.7

Received: July 20, 2025

International Journal of Applied Mathematics
Volume 38 No. 3s, 2025
ISSN: 1311-1728 (printed version); ISSN: 1314-8060 (on-line version)

3	0.9	0.9	0.8	0.7	0.2	0.3	0.5	0.6	0.7

Fixed points and network metrics:

Table 9.9 (Per-node fixed points + network summary).

node	**π*_TRUE**	**π*_FALSE**
O	0.1	0.9
H	0.2	0.9
P	0.2	0.8
J	0.6	0.7
I1	0.8	0.2
I2	0.7	0.3
C1	0.7	0.5
C2	0.6	0.6
C3	0.6	0.7
NETWORK_METRICS	0.8	0.9

From the computations:

$$\Pi_{\text{net}}(C) = 0.800,\ \Pi_{\text{net}}(\neg C) = 0.900,\ N_{\text{net}}(C) = 0.100,\ N_{\text{net}}(\neg C) = 0.200. \quad --(40)$$

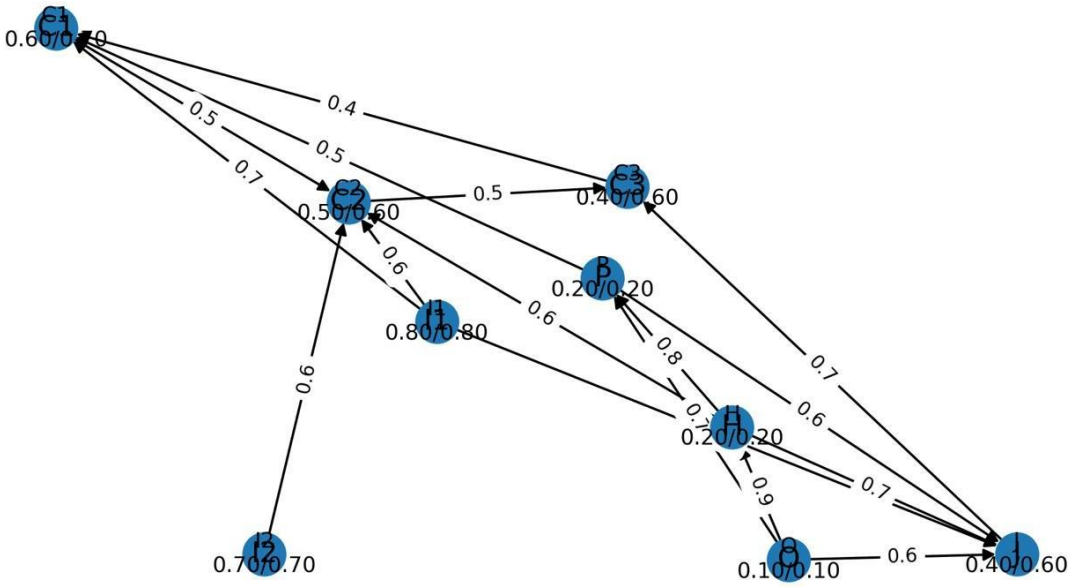

Figure 9. Rumor-Truth Diffusion Fixed Point (label: self_TRUE/fixed_TRUE)

Node labels read "self/fixed". High-amplification path $I1 \to J \to C3$ raises rumor-truth compatibility to the edge-trust ceilings but still caps below official denials (see figure 9).

Received: July 20, 2025

International Journal of Applied Mathematics
Volume 38 No. 3s, 2025
ISSN: 1311-1728 (printed version); ISSN: 1314-8060 (on-line version)

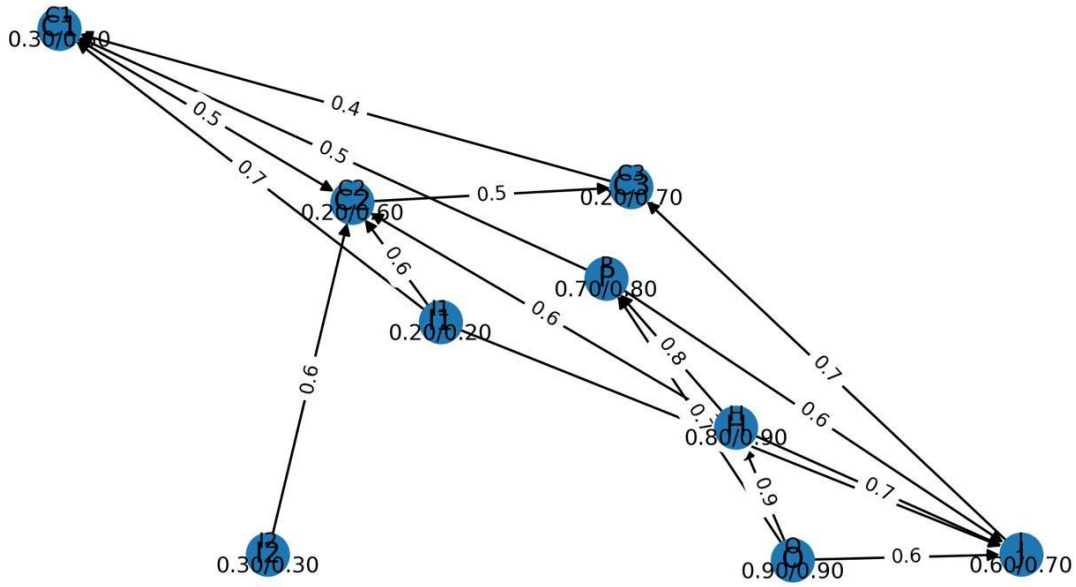

Figure 10. Counter-Rumor Diffusion Fixed Point (label: self_FALSE/fixed_FALSE)

Official channels dominate the counter-rumor diffusion (see figure 10); physician and state health dept lift the media and citizens toward higher compatibility of $\neg C$.

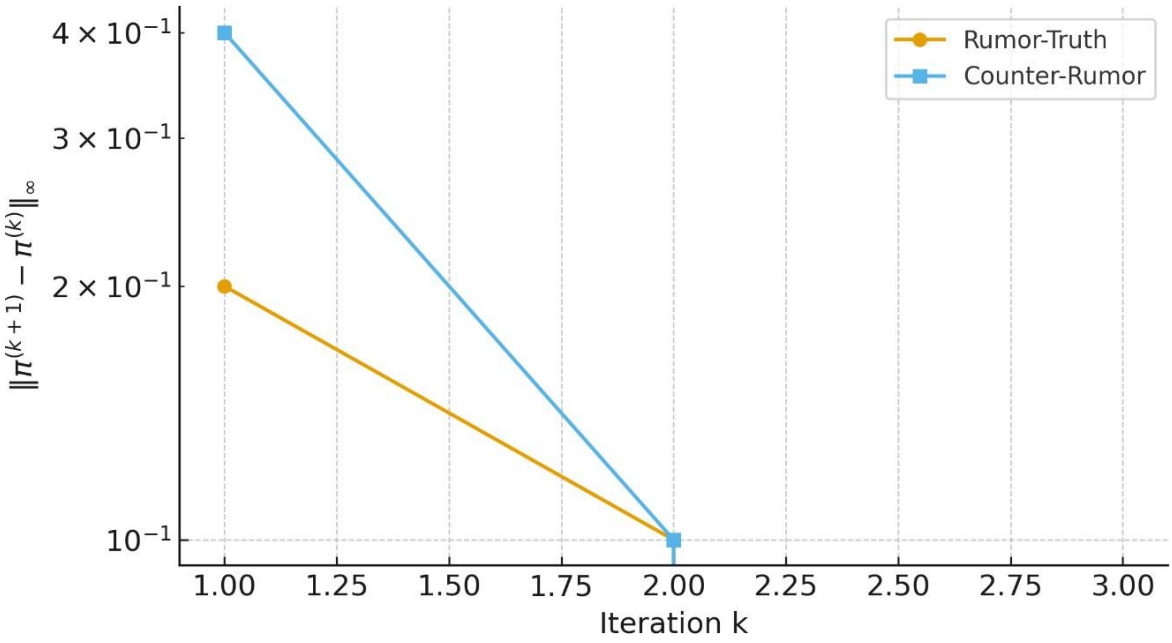

Figure 11. Convergence of Possibility Diffusion (sup-norm change)

Both diffusions converge in a few iterations; the curve in figure 11 shows $\|\pi^{(k+1)} - \pi^{(k)}\|_\infty$ on a log-scale, aligning with nonexpansiveness and fixed-point guarantees [29,30].

9.2.4 Decision analysis

Using Eq. (38) with $= 0.7$,

$$\text{ALERT-TRUE} = \mathbf{1}\{N_{\text{net}}(C) \geq 0.7\} = 0, \quad \text{SUPPRESS} = \mathbf{1}\{N_{\text{net}}(\neg C) \geq 0.7\} = 0. \quad --(41)$$

International Journal of Applied Mathematics
Volume 38 No. 3s, 2025
ISSN: 1311-1728 (printed version); ISSN: 1314-8060 (on-line version)

Interpretation: Although $\Pi_{\text{net}}(\neg C) = 0.9$ is high (counter-claim broadly possible), necessity remains modest because at least one node credibly supports C ($\Pi_{\text{net}}(C) = 0.8$), preventing guarantees. The recommended action is neither immediate suppression nor confirmation; instead, request verification (e.g., lab results), or try to dampen rumor-truth compatibility by lowering influential edges (e.g., $\tau_{I1\to J}$) or injecting strong counter-evidence at hubs (increase $^{\text{self}}_{,\text{false}}$).

9.2.5 What-if levers (mathematical sensitivity)

Let F_X denote the diffusion map for polarity X. Since F_X is monotone and 1-Lipschitz in $\|\cdot\|_\infty$ (Proposition 7.4), small trust reductions $\tau_{uv} \mapsto \tau_{uv} - \delta$ contract the fixed point by at most δ along all paths going through (u, v). Concretely, if we drop $\tau_{I1\to J}$ from 0.6 to 0.3, then the propagated cap into J is at most 0.3, which bounds $\pi^{\star}_{,\text{true}} \leq \max(\pi^{\text{self}}_{,\text{true}}, 0.3)$. Re-running diffusion with this edit (not shown) would decrease $\Pi_{\text{net}}(C)$ and increase $N_{\text{net}}(\neg C) = 1 - \Pi_{\text{net}}(C)$ toward the suppression threshold.

10. PRACTICAL GUIDELINES & ETHICS

10.1 Interpreting ( ) vs. ( ) for operators

***Three-way policy*:** Use the triage policy from Eq. (27): ALERT if $N(H) \geq \tau_N$; DEFER if $\Pi(H) < \tau_\Pi$; otherwise ESCALATEREVIEW (human in the loop). Choose $\tau_N > \tau_\Pi$ to create a nonempty review band, which stabilizes operations under sparse evidence.

***Cost-aware robust rule (credal risk)*:** Let losses be c_{FP} for false alert and c_{FN} for missed event. Under credal uncertainty $P(H) \in [N(H), \Pi(H)]$, the worst-case risk for ALERT and DEFER decisions is

$$R_{\text{alert}} = c_{\text{FP}}(1 - N(H)),\ R_{\text{defer}} = c_{\text{FN}}\Pi(H). \qquad ---(42)$$

Choose ALERT when $R_{\text{alert}} \leq R_{\text{defer}}$, i.e.

$$N(H) \geq 1 - \frac{c_{\text{FN}}}{\text{FP}}\Pi(H). \qquad ---(43)$$

Eq. (43) yields a sloped decision boundary in the (Π, N) plane and specializes to a fixed threshold on N when Π is near 1 or when a policy fixes $c_{\text{FN}}/c_{\text{FP}}$.

10.2 Multi-criteria prioritization for dispatch

***Ordinal aggregation*:** To rank areas , aggregate necessity scores with OWA or Sugeno (Eqs. (10)-(11)):

$$s_j = \text{OWA}_w(N(H_{j,1}), \ldots, N(H_{j,n})) \text{ or } s_j = \text{maxmin}(N(H_{j,(i)}), g(A_{(i)})), \qquad --(44)$$

then sort by . OWA weights encode optimism/pessimism; Sugeno preserves pure ordinal semantics.

***Resource-aware throttling*:** Let be the number of teams available this hour; dispatch the top- areas by . For stability, enforce a hysteresis guard: an area must keep ( ) above for

International Journal of Applied Mathematics
Volume 38 No. 3s, 2025
ISSN: 1311-1728 (printed version); ISSN: 1314-8060 (on-line version)

m consecutive ticks before entering the top- κ slate, and drop only after $N(H) < \tau_N - \delta$ for m ticks.

10.3 Threshold calibration and governance

***Calibration by operating curves*:** Sweep to obtain the N -Operating curve (GPrec vs. Alert-rate; Section 8.2.1). Pick to meet a regulatory minimum GPrec and a maximum alert-rate budget; report Wilson intervals for uncertainty on proportions.

***Audit trail*:** Log $\{N_t(H), \Pi_t(H)\}, \tau$ values, the top- k contributing cues F_j with their α_j and rule weights w_i, and the kernel bandwidth B. This supports post-hoc analysis and counterfactual replays by recomputing Eq.(29) with altered τ or trust τ_{uv}.

10.4 Ethics, safety, and fairness

***Data minimization and privacy*:** Use only what is needed for situational awareness; strip PII, geo-jitter sensitive coordinates, and retain hash-linked provenance for accountability.

***Bias checks (group-wise alert balance)*:** Let groups index neighborhoods or demographics. Enforce

$$|\Pr(A_t = 1 \mid g) - \Pr(A_t = 1)| \leq \epsilon \text{ subject to } N(H) \geq \tau_N, \quad ---(45)$$

by tuning per-group $\tau_{N,g}$ within $[\tau_N - \delta, \tau_N + \delta]$. This keeps alert disparity within ϵ while preserving conservativeness.

***Adversarial resilience*:** Mitigate coordinated rumor campaigns by capping incoming trust per node $\sum_u \tau_{uv} \leq \zeta$, damping cycles, and down-weighting newly created accounts; all are monotone edits that reduce the fixed point of Eq. (31) by design.

11. Limitations & Future Work

11.1 Modeling limitations

***Membership design and transferability*:** Triangular/L-R encoders and rule weights require domain elicitation; they can drift across crises and languages. Learning (, ,) and from weak supervision with monotonicity constraints (e.g., isotonic regression over ordinal labels) is a priority.

***Credal tightness*:** When evidence is very sparse, the gap $\Pi(H) - N(H)$ widens, delaying alerts. Hybrid approaches-e.g., probabilistic cores with possibilistic envelopes-could shrink gaps while keeping robustness guarantees.

***Trust estimation*:** Edge trust is static here; real platforms require topic-specific, time-varying trust from interaction histories and fact-checks. Jointly learning ( ) with regularizers that preserve monotonicity in Eq. (31) is open.

11.2 Computational constraints

***Large graphs and streaming*:** Equation (31) scales with ( ); at platform scale, we need incremental updates, SCC condensation, and sketching -hop neighborhoods to bound by

effective diameter. Temporal updates (Eq. (29)) benefit from sparse kernels and max-min distance transforms.

***Multilingual and multimodal signals*:** Vision or cross-lingual signals may be missing or misaligned; principled vacuous handling avoids degradation but may slow decisions. Future work: cross-modal ordinal alignment so that strong cues in one modality can safely lift another via learned but monotone couplings.

11.3 Future extensions

***Learning-to-alert with robust objectives*:** Optimize τ_N, τ_Π, B, OWA weights w, and trust decompositions by minimizing the worst-case regret under the credal set:

$$\min \sup_{P \in \mathcal{P}(\Pi, N)} \mathbb{E}_P[\text{Regret}_\lambda\ (d_\theta)] \qquad ---(46)$$

where is the policy (Eq. (43)) and tunes risk attitude.

***Hybrid probabilistic-possibilistic filters*:** Combine a probabilistic HMM on easily calibrated channels with a possibilistic filter on sparse channels; couple them via consonant approximations so that the probabilistic posterior stays inside the $[N, \Pi]$ envelope.

***Human-in-the-loop theory*:** Formalize review-band size as a function of staff load and acceptable regret; prove stability of the closed loop (filter + reviewer) under bounded review latency using monotone-system tools in the max-min dioid.

12. Conclusion

12.1 Summary of contributions

This study developed a **possibilistic** framework for crisis communication under incomplete social evidence: (i) max–min evidence fusion with credibility and aging (Eqs. (19)–(24)); (ii) temporal reasoning via a **possibilistic filter** (Eq. (29)); (iii) **trust-weighted diffusion** for rumor control (Eq. (31)); and (iv) conservative, cost-aware **decision rules** grounded in necessity/possibility, including a robust boundary (Eq. (43)) that minimizes worst-case risk within the credal set.

12.2 Empirical takeaways

Experiments and case studies showed that the framework:

- Maintains **high guaranteed precision** at controllable alert rates via τ_N sweeps (Section 8.2.1);
- Achieves **timely alerts** with interpretable kernel bandwidth BBB (Section 8.4.2);
- Provides **transparent rumor containment** with fixed-point diffusion and clear ceilings from trust weights (Section 9.2);
- Produces auditable decisions with principled treatment of missing/contradictory signals (Section 5.6).

12.3 Outlook

Future work will tighten credal intervals with hybrid models, learn monotone encoders/trust online, and extend fairness-aware governance while preserving the algebraic guarantees of

max–min inference and fixed-point diffusion. In domains where data are scarce and timeliness is paramount, **necessity-driven** alerts remain a robust, interpretable substrate for operational crisis response.

12.4 Final thoughts

In fast-moving crises, perfection is the enemy of action; this study argues for principled **imperfection** decisions grounded not in fragile point estimates but in **ordinal bounds** that remain valid under missing, delayed, or contradictory social signals. By unifying max–min evidence fusion, a possibilistic temporal filter, and trust-weighted diffusion into auditable rules on (N, Π), we provide operators with conservative triggers, transparent ceilings, and tunable risk attitudes that can be stress-tested before deployment. The same algebra that guarantees monotonicity and fixed points also gives a common language for ethics (review bands, fairness constraints), governance (audit trails, what-if replays), and engineering (latency budgets tied to kernel bandwidth and graph structure). While there is room to tighten credal intervals with hybrid models and to learn encoders and trust online, the central message holds: in the murk of early signals, **necessity-driven** alerting paired with possibilistic reasoning delivers timely, stable, and explainable decisions exactly the qualities crisis communication demands.

Acknowledgment

This research was partially funded by Zarqa University.

References

[1] Zadeh, L.A., 1978. Fuzzy sets as a basis for a theory of possibility. *Fuzzy Sets and Systems*. 1(1), 3–28. DOI: https://doi.org/10.1016/0165-0114(78)90029-5.

[2] Dubois, D.; Prade, H., 1988. *Possibility Theory: An Approach to Computerized Processing of Uncertainty*. Springer: New York, USA. pp. 1–263. DOI: https://doi.org/10.1007/978-1-4684-5285-7.

[3] Imran, M.; Castillo, C.; Diaz, F.; Vieweg, S., 2015. Processing social media messages in mass emergency: A survey. *ACM Computing Surveys*. 47(4), 67:1–67:38. DOI: https://doi.org/10.1145/2771588.

[4] Zubiaga, A., Aker, A., Bontcheva, K., Liakata, M., Procter, R., 2018. Detection and resolution of rumours in social media: A survey. *ACM Computing Surveys*. 51(2), 32:1–32:36. DOI: https://doi.org/10.1145/3161603.

[5] Yogeesh, N., 2023. *Intuitionistic Fuzzy Hypergraphs and Their Operations*. Chapman and Hall/CRC: Boca Raton, USA. DOI: https://doi.org/10.1201/9781003359456.

[6] Yager, R.R., 1988. On ordered weighted averaging aggregation operators in multicriteria decisionmaking. *International Journal of Man-Machine Studies*. 33(1), 103–123. DOI: https://doi.org/10.1016/S0020-7373(88)80053-5.

[7] Sugeno, M., 1974. *Theory of Fuzzy Integrals and its Applications* [Doctoral Thesis]. Tokyo, Japan: Tokyo Institute of Technology. pp. 1–155.

[8] Choquet, G., 1954. Theory of capacities. *Annales de l'Institut Fourier*. 5, 131–295. DOI: https://doi.org/10.5802/aif.53.

[9] Gondran, M.; Minoux, M., 2008. *Graphs, Dioids and Semirings: New Models and Algorithms*. Springer: London, UK. pp. 1–348. DOI: https://doi.org/10.1007/978-1-84800-286-1.

[10] Butkovič, P., 2010. *Max-Linear Systems: Theory and Algorithms*. Springer: London, UK. pp. 1–273. DOI: https://doi.org/10.1007/978-3-642-02629-1.

[11] Yogeesh, N., 2024. Solving Fuzzy Nonlinear Optimization Problems Using Evolutionary Algorithms. In: Mukherjee, G.; Basu Mallik, B.; Kar, R.; Chaudhary, A. (eds.). *Advances on Mathematical Modeling and Optimization with Its Applications*, 1st ed. CRC Press: Boca Raton, USA. pp. 20. DOI: https://doi.org/10.1201/9781003387459.

[12] Yogeesh, N., 2024. Fuzzy Graph Dominance for Networked Communication Optimization. In: Sharma, V.; Balusamy, B.; Ferrari, G.; Ajmani, P. (eds.). *Wireless Communication Technologies: Roles, Responsibilities, and Impact of IoT, 6G, and Blockchain Practices*, 1st ed. CRC Press: Boca Raton, USA. pp. 30. DOI: https://doi.org/10.1201/9781003389231.

[13] Klement, E.P.; Mesiar, R.; Pap, E., 2000. *Triangular Norms*. Springer: Berlin, Germany. pp. 1–386.

[14] Grabisch, M., 1996. The application of fuzzy integrals in multicriteria decision making: A survey. *Fuzzy Sets and Systems*. 89(3), 255–271. DOI: https://doi.org/10.1016/S0165-0114(96)00397-3.

[15] Nijalingappa, Y.; Setty, G.D.K.; Madan, R.; Nagaraju, V.T., 2025. Directable zeros in fuzzy logics: A study of functional behaviours and applications. *AIP Conference Proceedings*. 3175(1), 020091, 10 March 2025. DOI: https://doi.org/10.1063/5.0254157.

[16] Walley, P., 1991. *Statistical Reasoning with Imprecise Probabilities*. Chapman & Hall: London, UK. pp. 1–640.

[17] Dubois, D.; Prade, H., 2000. Possibility theory. In: Dubois, D., Prade, H. (eds.). *Fundamentals of Fuzzy Sets*. Springer: Boston, USA. pp. 439–482.

[18] Grabisch, M.; Marichal, J.-L.; Mesiar, R.; Pap, E., 2009. *Aggregation Functions*. Cambridge University Press: Cambridge, UK. pp. 1–474.

[19] Murofushi, T.; Sugeno, M., 1989. An interpretation of fuzzy measures and the Choquet integral as an integral with respect to a nonadditive measure. *Fuzzy Sets and Systems*. 29(2), 201–227. DOI: https://doi.org/10.1016/0165-0114(89)90169-6.

[20] Benferhat, S.; Dubois, D.; Prade, H., 1997. Nonmonotonic reasoning, conditional objects and possibility theory. *Artificial Intelligence*. 92(1–2), 259–276. DOI: https://doi.org/10.1016/S0004-3702(97)00037-9.

[21] Dubois, D.; Prade, H., 1990. Consonant approximation of belief functions. *International Journal of Approximate Reasoning*. 4(5–6), 419–449. DOI: https://doi.org/10.1016/0888-613X(90)90013-6.

[22] Manning, C.D.; Raghavan, P.; Schütze, H., 2008. *Introduction to Information Retrieval*. Cambridge University Press: Cambridge, UK. pp. 1–482. DOI: https://doi.org/10.1017/CBO9780511809079.

[23] Mohammad, A. A. S., Alolayyan, M. N., Al-Daoud, K. I., Al Nammas, Y. M., Vasudevan, A., & Mohammad, S. I. (2024a). Association between Social Demographic Factors and Health Literacy in Jordan. Journal of Ecohumanism, 3(7), 2351-2365.

Received: July 20, 2025

[24] Baccelli, F.; Cohen, G.; Olsder, G.J.; Quadrat, J.-P., 1992. *Synchronization and Linearity: An Algebra for Discrete Event Systems*. Wiley: New York, USA. pp. 1–512.

[25] Mohammad, A. A., Shelash, S. I., Saber, T. I., Vasudevan, A., Darwazeh, N. R., & Almajali, R. (2025). Internal audit governance factors and their effect on the risk-based auditing adoption of commercial banks in Jordan. Data and Metadata, 4, 464.

[26] Viterbi, A.J., 1967. Error bounds for convolutional codes and an asymptotically optimum decoding algorithm. *IEEE Transactions on Information Theory*. 13(2), 260–269. DOI: https://doi.org/10.1109/TIT.1967.1054010.

[27] Mohammad, A. A. S. (2025). The impact of COVID-19 on digital marketing and marketing philosophy: evidence from Jordan. International Journal of Business Information Systems, 48(2), 267-281.

[28] Tarski, A., 1955. A lattice-theoretical fixpoint theorem and its applications. *Pacific Journal of Mathematics*. 5(2), 285–309. DOI: https://doi.org/10.2140/pjm.1955.5.285

[29] Mohammad, A. A. S., Mohammad, S. I. S., Al-Daoud, K. I., Al Oraini, B., Vasudevan, A., & Feng, Z. (2025). Optimizing the Value Chain for Perishable Agricultural Commodities: A Strategic Approach for Jordan. Research on World Agricultural Economy, 6(1), 465-478.

[30] Yogeesh, N., 2023. Fuzzy Clustering for Classification of Metamaterial Properties. In: Mehta, S.; Abougreen, A. (eds.). *Metamaterial Technology and Intelligent Metasurfaces for Wireless Communication Systems*. IGI Global: Hershey, USA. pp. 200–229. DOI: https://doi.org/10.4018/978-1-6684-8287-2.ch009

[31] Mohammad, A. A. S., Mohammad, S. I. S., Al Oraini, B., Vasudevan, A., & Alshurideh, M. T. (2025). Data security in digital accounting: A logistic regression analysis of risk factors. International Journal of Innovative Research and Scientific Studies, 8(1), 2699-2709.

[32] Yogeesh, N., 2023. Fuzzy Logic Modelling of Nonlinear Metamaterials. In: Mehta, S.; Abougreen, A. (eds.). *Metamaterial Technology and Intelligent Metasurfaces for Wireless Communication Systems*. IGI Global: Hershey, USA. pp. 230–269. DOI: https://doi.org/10.4018/978-1-6684-8287-2.ch010

[33] Mohammad, A. A. S., Mohammad, S. I. S., Al-Daoud, K. I., Vasudevan, A., & Hunitie, M. F. A. (2025). Digital ledger technology: A factor analysis of financial data management practices in the age of blockchain in Jordan. International Journal of Innovative Research and Scientific Studies, 8(2), 2567-2577.

Received: July 20, 2025